

## Supplementary Information

### A New Strain-Crystallizable Rubber via Neodymocene-Catalyzed Regio-, Stereo-, and Sequence-Selective Copolymerization of Isoprene and Ethylene

Jingqing Lyu,<sup>a</sup> Zhenxing Chen,<sup>b</sup> Lei Zhu,<sup>b,\*</sup> and Li Jia<sup>a,\*</sup>

<sup>a</sup>School of Polymer Science and Polymer Engineering, The University of Akron, Akron, Ohio 44325-3909

<sup>b</sup>Department of Macromolecular Science and Engineering, Case Western Reserve University, Cleveland, Ohio 44106-7202

1. Experimental Details including polymerization procedures, instruments and techniques for characterization, and tensile testing method (pp S2 – S6).
2. Figure S1. <sup>1</sup>H and <sup>13</sup>C{<sup>1</sup>H} NMR spectra of the products from entry 1 (IER-82) in Table 1 in CDCl<sub>3</sub> at room temperature. (p S7)
3. Figure S2. DSC traces of IERs with different structural regularities. (p S7)
4. Figure S3. DSC study of crystallization and melting of uncured IER-95. (p S8)
5. Figure S4. WAXD of DCP-cured IER-95 crystallized at -40 °C for 4h in the absence of any strain. (p S8)
6. Figure S6. 2D WAXD pattern of DCP-cured IER-95 at -25 °C at 200%, 600% and 800% strains. (p S9)
7. Figure S5. WAXD azimuthal analysis for degree of orientation for strain-induced crystal at 200% and 600% (p S9).
8. Table S1. Density of elastically effective strands of rubber samples used in this study. (p S10)
9. Table S2. Assignment of Miller indices to the observed diffractions and comparison of the observed d-spacings and the calculated d-spacings using the monoclinic unit cell parameters (a = 2.21 nm, b = 0.72 nm, c = 1.30 nm, and β = 110.8°). (p S10)
10. Table S3. Summary of tensile properties. (p S11)
11. References. (p S11)

## Experimental Details

**General Methods.** All reactions were carried out under a dry and oxygen-free nitrogen atmosphere using Schlenk techniques or in an MBraun glovebox. All solvents were purchased from Sigma Aldrich and dried using an MBraun solvent purification system. All other chemicals were purchased from Sigma Aldrich or VWR.  $\text{Bu}_2\text{Mg}$  was used after the solvent was removed from its solution (1 M in heptane). Isoprene was dried by dibutyl magnesium. Ethylene (99.9% from Linde) was used without further purification. Neodymocenes **1** - **3** were synthesized following the procedures in the literature.<sup>1-2</sup>

**Copolymerization.** Catalyst **1**, **2**, or **3** and, if necessary,  $\text{Bu}_2\text{Mg}$  were added to an autoclave in the glove box. Isoprene was added using a syringe into an autoclave connected to a Schlenk line under a gentle flow of nitrogen. Ethylene was introduced to the autoclave until the desired pressure was reached. The autoclave was stirred at room temperature with a magnetic stirrer for a given period or placed in an oil bath at a set temperature and stirred. The pressure was released in a well-ventilated fume hood, and the autoclave was opened. Methanol (100 mL) was poured into the autoclave to precipitate the product. The product was placed in a glass contained and dried under vacuum at room temperature. See Table 1 for the specific amounts of catalyst and isoprene and the ethylene pressure as well as the reaction temperature and time for each run.

**Nuclear Magnetic Resonance (NMR).**  $^1\text{H}$  NMR spectra were recorded with an Agilent Mercury 300 MHz instrument. Quantitative  $^{13}\text{C}$  NMR spectra were recorded with an Agilent Mercury 500 MHz instrument equipped with an inverse probe. All spectra were taken at room temperature in deuterated solvents. The solvent peak was used as the reference for chemical shifts.

For quantitative  $^{13}\text{C}\{^1\text{H}\}$  NMR, the pulse sequence for inverse gated  $^1\text{H}$  decoupling was used to eliminate NOE. Sufficient delay between pulses was insured by acquiring two spectra using different delay times (5 and 10 seconds) and observing the same integration ratios. The integrations of the methyl groups in the various isoprene-containing repeat units (i.e., 1,4-trans-isoprene-ethylene, 1,4-cis-isoprene-ethylene, 3,4- isoprene-ethylene, and repetitive isoprene units if present) and the  $\text{CH}_2$  group of the repetitive ethylene units if present were used to quantify the abundances of these repeat units.

**Gel permeation chromatograph (GPC).** GPC was performed on a Tosoh HLC-8320 GPC having two TSK-GEL SuperH3000 columns and one TSK-GEL SuperH5000 column equipped with a refractive index detector. THF was used as the eluent at a flow speed of 0.350 ml/min at 40 °C. Molecular weights were determined relative to polystyrene standards.

**Differential Scanning Calorimetry (DSC).** A TA Instruments Discovery DSC250 was used. The instrument was equipped with an RCS 90 cooler with a low temperature limit of about -85 °C, which can only be reached slowly toward the end. To obtain the glass transition temperature due to the cooling rate limitation, the sample was cooled to -85 °C first without recording the heat flow during the cooling process. The sample was held isothermally for 3 min at -85 °C. The temperature was then raised at the rate of 10 °C/min from -85 °C to 100 °C, and the heat flow was recorded. Two cooling-heating cycles were carried out, and they were identical. The DSC traces of the second heating ramps are shown in Figure S1. To study the thermal crystallization and melting, the sample was held isothermally at either -40 °C and -20 °C for 4 h before the temperature scan started at the rate of 10 °C/min as shown in Figure S2.

**Curing and Preparation of Cured Specimens.** Dicumyl peroxide (DCP) was incorporated into the polymer matrix using a two-roll mill at 40 °C. The resulting compound was

then cured in a hydraulic press at 160 °C for 30 minutes to form a rubber sheet with the dimensions of  $63.5 \times 63.5 \times 1.0$  mm. Dumbbell specimens were cut out from the cured sheets with a die in accordance with ASTM D638 Type V specifications ( $63.5 \times 3.0 \times 1.0$  mm, the width and thickness were measured from the middle section of the dumbbell). The specimens were used for subsequent mechanical studies.

**Determination of the Crosslinking Density.** The crosslinking density of the DCP-cured rubber was determined using both the method based on the Flory-Rehner equation and the method based on the Mooney Rivlin equation. For the former, a small piece of the DCP-cured scrap was cut out, weighed, and placed in toluene. The sample was weighed periodically. After a constant weight was reached, the density of elastic strands was calculated using the Flory-Rehner equation. The mass densities of all samples were taken as  $1.0 \text{ g/cm}^3$ . The  $\chi$  parameter of IER in toluene was assumed to be 0.40 because the  $\chi$  parameters of all common hydrocarbon elastomers in toluene fall in the narrow range of 0.35 – 0.49.<sup>3</sup> The results are summarized in Table S1. The data between 10% - 50% strain from the stress-strain curves at room temperature were plotted according to the Mooney-Rivlin equation. The results are summarized in Table S1.

**SIC study by Stress Relaxation and Recovery.** A Dynamic Mechanical Analyzer (DMA, TA RSA-G2) equipped with a liquid nitrogen cooling system was used for stress-relaxation and stress-recovery studies. The sample chamber was cooled to the desired temperature, and a rectangular specimen ( $\sim 5$  mm in length) cut out from the middle section of a dumbbell (i.e.,  $3 \times 1$  mm in width and thickness) was fixed between the clamps. After the chamber was closed for 15 min to allow the temperature of the sample to equilibrate, the clamp distance was adjusted to eliminate any stress. The sample was then extended to the desired strain, and the stress was monitored as a function of time. After the stress reached zero or at least lowered to below 50% of

the initial value, the sample was warm at the rate of 1 °C/min to allow stress to recover. The stress was recorded for at least another 10 min after it reached a plateau value before the experiment was stopped.

**Tensile Test.** An Instron 5567 with a temperature-controlled chamber with liquid nitrogen cooling system was used. The test was carried out with a 100N static load cell. The sample chamber was first taken to the desired temperature. Then, a Dumbbell specimen (63.5 x 3.0 x 1.0 mm) was fixed between the clamps. The chamber was then closed, the sample was kept for 15 min, and the clamp distance was adjusted so that the stress was zero. The sample was extended to break at the strain rate of 20%/min. The results are summarized in Table S3.

**Wide Angle X-Ray Diffraction Measurement.** All X-Ray experiments were carried out with a Xeuss 3.0 system equipped with a copper rotating anode emitting X-rays with a wavelength  $\lambda$  of 1.5418 Å (Cu K $\alpha$ ), an Eiger detector with a pixel size of 75  $\mu\text{m} \times 75 \mu\text{m}$ . The sample-to-detector distance was 52 mm. A Linkam Modular Force Stage, which allows a maximum strain of 300%, was used to hold the sample at a certain strain for the WAXD experiment. Due to the strain limit of the stage, for the experiments with the samples extended to 600% and 800% strains, the samples were pre-stretched to 300% and 400% strains, respectively, before being secured on the in situ stage. After the sample was secured, the extension stage with the sample was placed in the X-ray chamber, and the temperature was lowered at a rate of 10 °C/min. In 10 mins after the target temperature was reached, the sample was stretched to the desired strain and then kept at the specific temperature and strain for 2 h before collection of the scattering data. 2D scattering patterns were plotted using XSACT software. The 2D scattering intensity was integrated over all azimuthal angles with Xenocs software to give the 1D plot of scattering intensity as a function of the scattering angle  $2\theta$ .

The degree of orientation of strain-induced crystals was analyzed at 200% and 600% strain (Figure 4.17). The diffraction at  $2\theta = 19.28^\circ$  was used for the azimuthal analysis. The azimuthal angle-intensity plots reveal that the peak for the 600% strain pattern is noticeably sharper and narrower than that for 200% strain. The Herman's orientation factor (H) was determined to be -0.44 at 600% strain, approaching the theoretical limit of -0.5; whereas H is -0.31, indicating a lower degree of orientation. These results demonstrate that higher strain induces greater molecular alignment, leading to a more aligned strain-induced crystalline structure as expected.

**Unit Cell Determination.** In order to accurately locate the center of the diffractions for unit cell determination, the amorphous background, which was obtained with the sample at room temperature in the absence of any, was subtracted from the 2D pattern of the sample at 800% strain and  $-25^\circ\text{C}$ . The unit cell dimensions ( $a = 2.21\text{ nm}$ ,  $b = 0.72\text{ nm}$ ,  $c = 1.30\text{ nm}$ , and  $\beta = 110.8^\circ$ ) were determined from the background-subtracted fiber pattern. The calculated  $d$ -spacings and the observed  $d$ -spacings are compared in Table S2. They match very well with each other. The 12 chains per cell is calculated using the following expression based on the assumption that the crystal density is  $\sim 1\text{ g/cm}^3$ , similar to trans-polyisoprene and polyethylene:

$$N = \frac{\rho V}{M} N_A$$

where  $N$  is the number of chains per unit cell,  $\rho = 1\text{ g/cm}^3$ ,  $M = 96\text{ g/mol}$  is the molecular weight of the isoprene-ethylene repeat unit, and  $N_A$  is the Avogadro number.

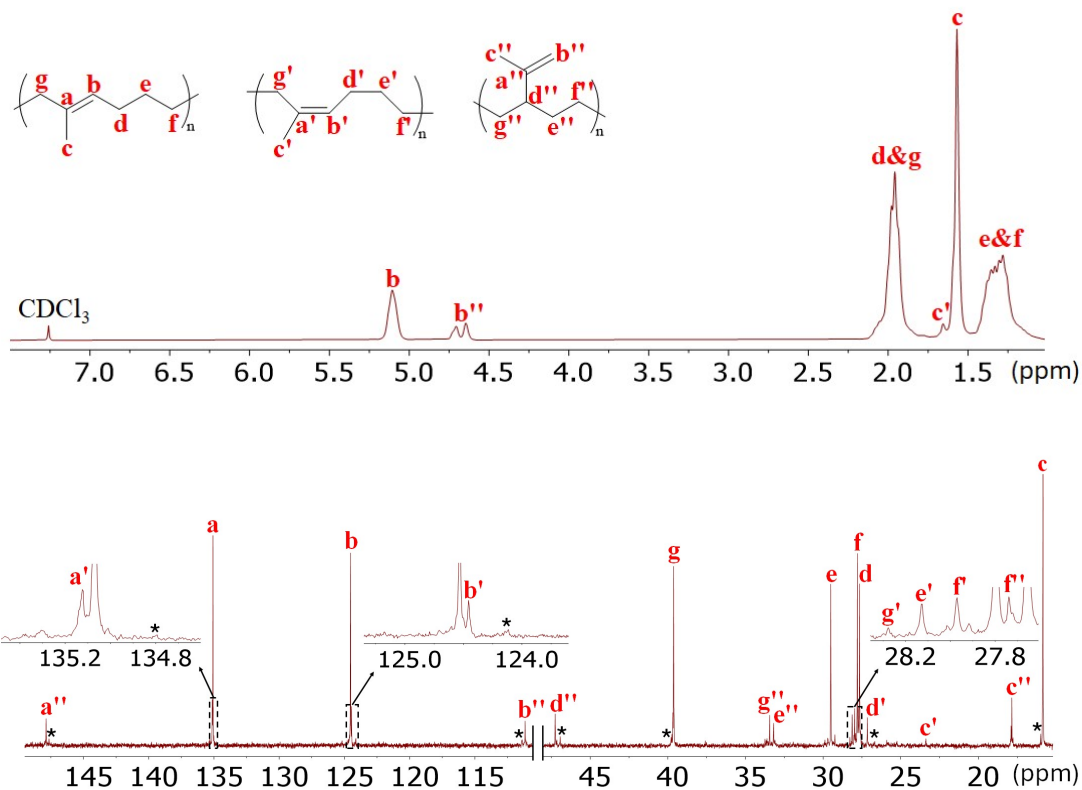


**Figure S1.**  $^1\text{H}$  and  $^{13}\text{C}\{^1\text{H}\}$  NMR spectra of the products from entry 1 (IER-82) in Table 1 in  $\text{CDCl}_3$  at room temperature. The peaks labeled with an asterisk belong to repetitive isoprene units.

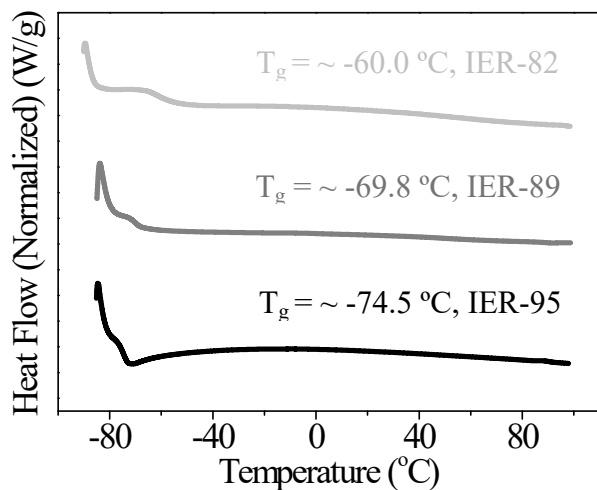


**Figure S2.** DSC traces of IERs with different structural regularities. The heating rate is  $10^{\circ}\text{C}/\text{min}$ .

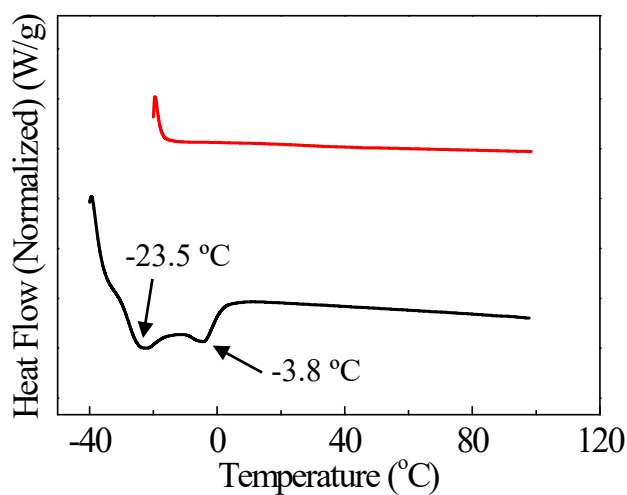


**Figure S3.** DSC study of crystallization and melting of uncured IER-95. The samples were held isothermally at  $-40\text{ °C}$  (black line) and  $-20\text{ °C}$  (red line) for 4 h before the temperature was increased at the rate of  $10\text{ °C/min}$ .

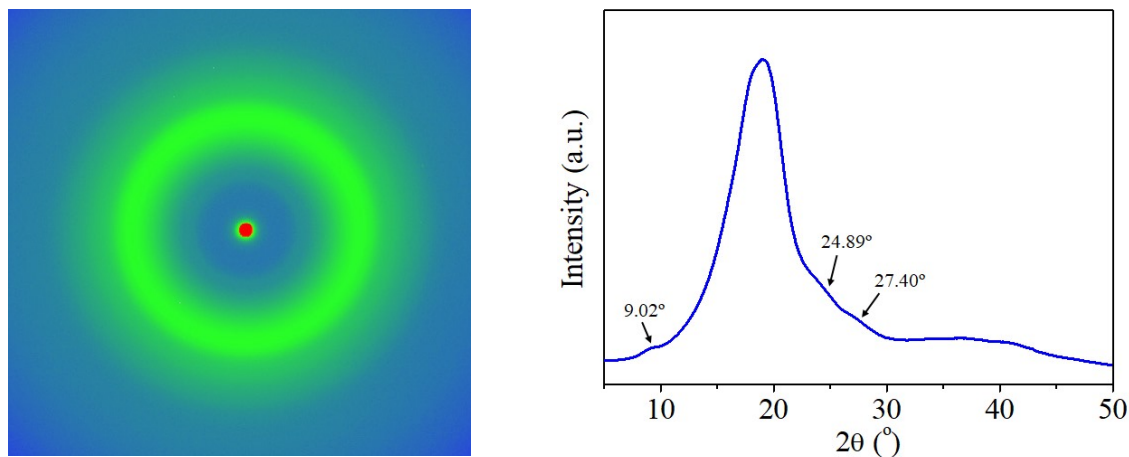


**Figure S4.** WAXD of DCP-cured IER-95 crystallized at  $-40\text{ °C}$  for 4h in the absence of any strain. Left: 2D pattern. Right: 1D plot of scattering intensity vs  $2\theta$ . The scattering intensity was integrated over all azimuthal angles.

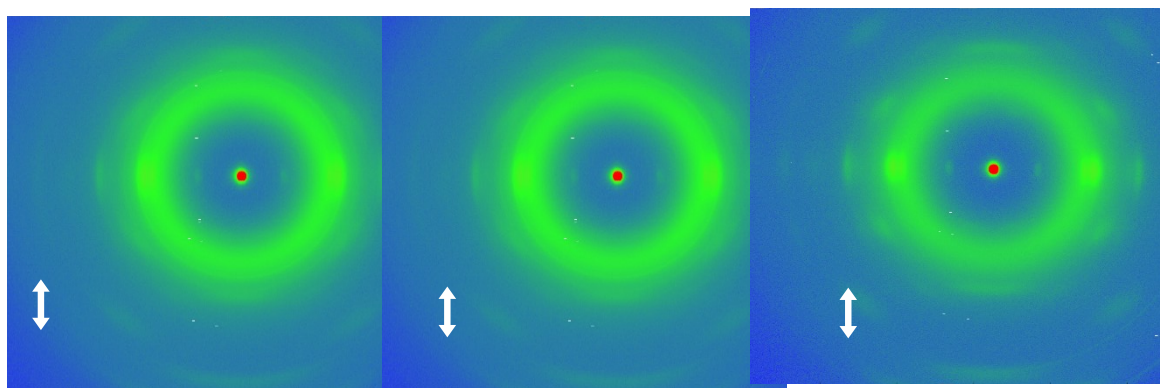


**Figure S5.** 2D WAXD pattern of DCP-cured IER-95 at -25 °C at 200%, 600% and 800% strains from left to right.

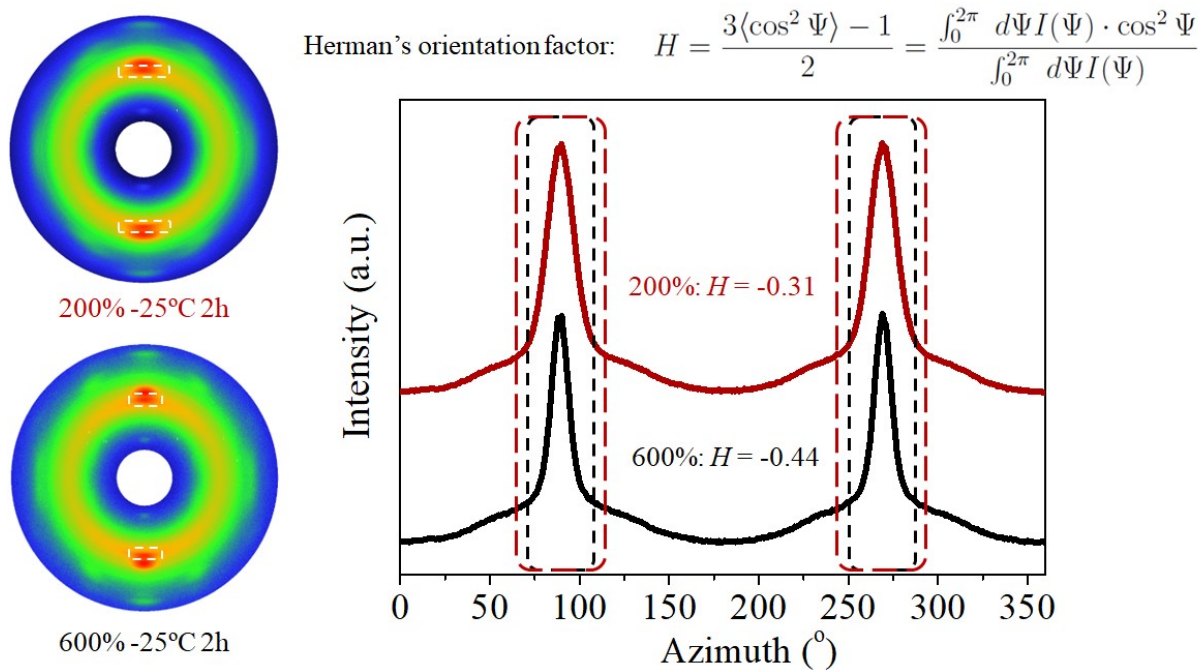


**Figure S6.** WAXD azimuthal analysis for degree of orientation for strain-induced crystal at 200% and 600%.

**Table S1.** Density of elastically effective strands of rubber samples used in this study.

Entry	Rubber	$\nu$ (mol/m <sup>3</sup> ) Flory-Rehner	$\nu$ (mol/m <sup>3</sup> ) Mooney-Rivlin
1	NR	56.4	-
2	IR	57.9	52.2
3	IER-95	53.3	55.0
4	IER-89	55.7	56.5

**Table S2.** Assignment of Miller indices to the observed diffractions and comparison of the observed d-spacings and the calculated d-spacings using the monoclinic unit cell parameters ( $a = 2.21$  nm,  $b = 0.72$  nm,  $c = 1.30$  nm, and  $\beta = 110.8^\circ$ ).

$2\theta$ (°)	h k l	$d_{\text{obs}}$ (nm)	$d_{\text{cal}}$ (nm)
9.21	-1 0 1	0.916	0.916
12.46	-1 1 0	0.687	0.680
19.38	-2 0 2	0.458	0.458
21.10	3 0 3	0.422	0.421
24.84	0 2 0	0.354	0.360
24.84	-3 1 2	0.344	0.344
27.66	0 2 2	0.323	0.310
28.27	-3 0 3	0.303	0.305
35.55	-2 2 3	0.249	0.247
38.73	0 3 0	0.234	0.240
44.08	-3 3 2	0.213	0.205

**Table S3.** Summary of tensile properties.

Sample		$\sigma_b$ (MPa)	$\epsilon_b$ (%)	$\sigma_{100\%}$ (MPa)	$\sigma_{300\%}$ (MPa)	Toughness (MJ/m <sup>3</sup> )
RT	NR	15.3 ± 0.9	780 ± 10	1.00 ± 0.05	2.9 ± 0.1	43 ± 3
	IR	10.0 ± 0.5	730 ± 20	0.60 ± 0.01	1.54 ± 0.02	23.0 ± 2
	IER-95	1.9 ± 0.2	709 ± 4	0.58 ± 0.05	0.92 ± 0.08	7.4 ± 0.6
	IER-89	1.2 ± 0.1	337 ± 4	0.60 ± 0.06	1.1 ± 0.1	2.5 ± 0.3
0 °C	NR	17.2 ± 0.8	780 ± 10	1.25 ± 0.04	3.52 ± 0.1	49 ± 3
	IR	11.0 ± 0.6	730 ± 10	0.76 ± 0.03	1.78 ± 0.07	25 ± 2
	IER-95	14.7 ± 0.5	1140 ± 10	1.21 ± 0.04	1.89 ± 0.06	56 ± 3
	IER-89	2.8 ± 0.3	661 ± 6	0.74 ± 0.08	1.4 ± 0.2	10.3 ± 0.9

**Reference**

1. Rodrigues, A.-S.; Kirillov, E.; Vuillemin, B.; Razavi, A.; Carpentier, J.-F., Stereocontrolled styrene–isoprene copolymerization and styrene–ethylene–isoprene terpolymerization with a single-component allyl ansa-neodymocene catalyst. *Polymer* **2008**, *49* (8), 2039-2045.
2. Thuilliez, J.; Monteil, V.; Spitz, R.; Boisson, C., Alternating copolymerization of ethylene and butadiene with a neodymocene catalyst. *Angewandte Chemie* **2005**, *117* (17), 2649-2652.
3. Sheehan, C.; Bisio, A., Polymer/solvent interaction parameters. *Rubber Chemistry and Technology* **1966**, *39* (1), 149-192.